

Electron Energy Loss Vibrational Spectra of Cyclopropane on Cu(111): Negative Ion Formation at 6 eV

Richard Martel[†] and Peter McBreen*

Département de chimie, Université Laval, Québec G1K 7P4, Canada

Received: January 13, 1997; In Final Form: April 16, 1997[®]

High-resolution electron energy loss (HREELS) spectra of cyclopropane adsorbed on Cu(111) were recorded over a range of primary electron energies. Vibrational excitation functions mapped out over the 2–18 eV primary energy range reveal a shape resonance centered at approximately 6 eV. The internally normalized excitation functions permit a separation of the observed losses into two families of modes, one associated with ring vibrations and one with CH vibrations. Although all of the loss peaks draw intensity from the shape resonance, there is a preferential enhancement of the CH bands and, in particular, the CH stretching loss. The shape resonance is assigned to $4e'$ in D_{3h} symmetry on the basis of the excitation spectra and by reference to gas phase studies. By applying the selection rules appropriate for resonance scattering, the point group symmetry for adsorbed cyclopropane is determined to be either C_{3v} or $C_s(\sigma_v)$. Additional arguments are given in favor of a C_{3v} geometry.

Introduction

Cyclopropane ($c\text{-C}_3\text{H}_6$) displays properties intermediate between those of alkanes and alkenes. For example, it has the strongest CH bond (106.3 kcal/mol) of all alkanes, and its CC bond energy is low due to ring strain (27.5 kcal/mol).^{1,2} The relatively high reactivity of cyclopropane, compared to that for straight chain alkanes, results in its use as a simple probe molecule for studying issues related to reaction mechanisms and selectivity in supported metal catalysis.³ Its frontier orbitals may be viewed as arising from the combination of three sp^2 hybrids located on the methylene groups.⁴ The σ - and π -type combination of these orbitals yields the so-called internal and external ring orbitals, respectively, with the external $3e'$ pair being the highest occupied levels. The partly π character of the CC bonds accounts for the similarity to ethylene.¹ Recent calculations support the appropriateness of a bent bond description and also underline the similarity to the CC bond in ethylene.¹ Adsorbed ethylene is one of the best studied systems in surface science,⁵ but there is very little spectroscopic information available on $c\text{-C}_3\text{H}_6$ adsorption on single crystal surfaces. Cyclopropane is known to undergo low-temperature dissociation on the reconstructed Ir(110)-(1 \times 2)⁶ surface and CC bond cleavage by reaction with bulk hydrogen on Ni(100).⁷ However, cyclopropane desorbs molecularly from clean Ru(0001),⁸ Ru(1120),⁹ Cu(100),¹⁰ Cu(110),¹¹ and Ni(100)⁷ in the 125–155 K range.

The present study deals with the interpretation of impact energy dependent high-resolution electron energy loss (HREELS) data for cyclopropane on Cu(111). In particular, the identification and analysis of a shape-resonance feature at 6 eV is used to determine the adsorption symmetry, and supporting temperature programmed desorption (TPD) and HREELS data are used to compare the adsorption of cyclopropane on copper with that reported for other metal surfaces. Formation of a temporary negative ion by electron capture into an acceptor level typically manifests itself in an enhancement of the intensity of specific fundamental vibrational modes as well as the excitation of

combination and overtone bands.¹³ This enhancement results from the decay of the transient negative ion by autodetachment, leading to a vibrationally excited ground state of the neutral target molecule.¹⁴ Shape resonance formation may be detected in a HREELS experiment by measuring vibrational spectra over a range of impact energies and plotting appropriately normalized vibrational excitation functions.¹³ The resonant enhancement of specific vibrational modes depends on both the symmetry of the negative ion state and the antibonding nature of the acceptor orbital involved in resonant electron capture. Thus, by observing which modes draw intensity from the resonance, the point group symmetry of the adsorbed molecule may be determined by taking into consideration the symmetry of the negative ion state and using the selection rules formulated by Wong and Schultz.¹⁵

Since shape resonance excitation involves electron capture into an acceptor orbital, it can be used as a probe of acceptor levels that are located above the vacuum level. This is very important in relation to the thermal surface chemistry of $c\text{-C}_3\text{H}_6$ since, in contrast to linear alkanes, cyclopropane possesses a manifold of low-lying antibonding levels,¹⁶ thus making it more easily activated by electron transfer from the metal. In this experiment an external electron is transferred to the cyclopropane/metal system. As shown in a separate publication, nonthermal CC and CH bond cleavage in cyclopropane on copper occur through a dissociative electron attachment resonance at 10 eV.^{11,17} This paper, however, deals with the detection of a shape resonance at 6 eV for $c\text{-C}_3\text{H}_6$ on Cu(111).

Experimental Section

The experiments were performed in an ultrahigh-vacuum chamber at a base pressure of 2×10^{-10} Torr. The system was equipped for Auger, HREELS, and TPD measurements. A detailed description of the dispersion compensation type spectrometer used in this study is given in a series of papers by Kevan, and co-workers.^{18,19} The overall resolution in the DC-HREELS configuration is independent of the resolution of the monochromator, and this allows the delivery of a high current density to the sample without sacrificing the high-resolution capability of the instrument. In-specular measurements were made at 45° to the surface normal. Off-specular measurements

* To whom correspondence should be addressed.

[†] Present address: T. J. Watson Research Centre, IBM, Yorktown Heights, NY 10598.

[®] Abstract published in *Advance ACS Abstracts*, June 1, 1997.

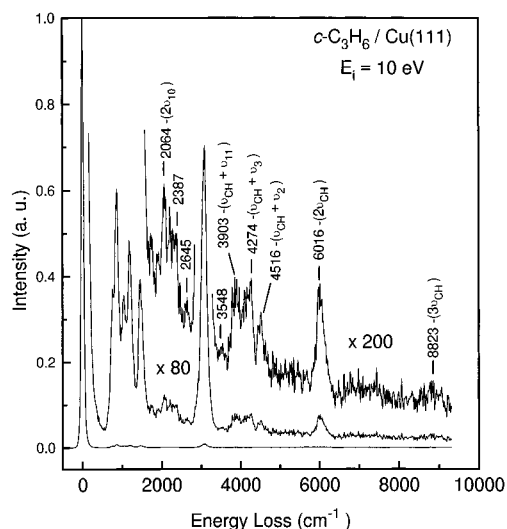


Figure 1. HREELS spectrum of cyclopropane on Cu(111) at 90 K. The spectrum displays several overtone and combination bands.

TABLE 1: Gas and Adsorbed Phase Vibrational Data for Cyclopropane^a

mode	symmetry D_{3h}	$c\text{-C}_3\text{H}_6$ gas ²¹ (cm^{-1})	$c\text{-C}_3\text{H}_6/\text{Cu}(111)$ (cm^{-1})	assignment
ν_6	a''_2	3086		
ν_{12}	e''	3072	3076	ν (CH)
ν_8	e'	3008		
ν_1	a'_1	3004		
ν_2	a'_1	1475	1470	CH_2 scissor
ν_9	e'	1429		
ν_3	a'_1	1196	1179	ring breathing
ν_{13}	e''	1183		CH_2 twist
ν_4	a''_1	1129		
ν_5	a'_2	1075		CH_2 wag
ν_{10}	e'	1029	1034	δ (ring) ns
ν_{11}	e'	863	872	δ (ring) s
ν_7	a''_2	852		CH_2 rock
ν_{14}	e''	748	759	CH_2 twist

^a δ (ring), ring deformation; s, symmetric; ns, nonsymmetric.

were made by rotating the sample toward the analyzer. Typical values for the current on the sample and the resolution of the spectrometer were 10 nA and 8 meV, respectively.

The Cu(111) sample was cleaned by cycles of Ne^+ sputtering at room temperature and flash heating to 900 K. The cleanliness of the surface was monitored using AES and HREELS measurements before each experiment. Cyclopropane (Aldrich, 99% purity) was further purified using freeze, pump, and thaw cycles as verified by *in-situ* measurements using the mass spectrometer.

Results

Figure 1 displays a HREELS spectrum, acquired at an electron impact energy of 10 eV, for 1 langmuir exposure of cyclopropane to Cu(111) at 90 K. The observed loss frequencies are listed in Table 1 where they may be compared with data of the fundamental modes for gas phase cyclopropane.²⁰ (It may be helpful to consult the cyclopropane spectrum in Figure 6 where the frequencies of the fundamental modes are indicated.) It should be noted that the spectrum in Figure 1 displays relatively intense overtone and combination loss features. For example, losses which may be assigned to first and second CH stretch overtone transitions are observed at 6026 and approximately 8820 cm^{-1} , respectively. The signal to noise ratio for the second overtone band is, however, extremely weak. Additional measurements show that the loss intensities saturate at approximately

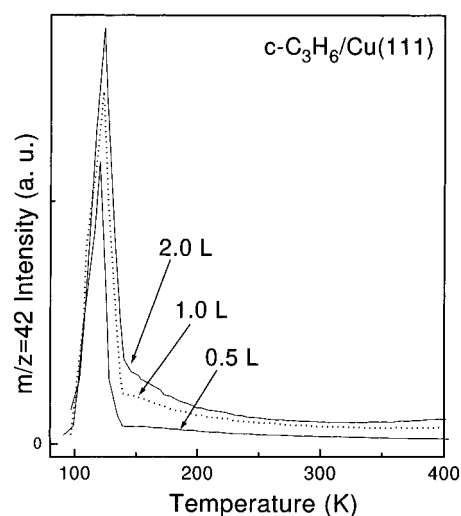


Figure 2. Thermal desorption data for $c\text{-C}_3\text{H}_6$ on Cu(111) as a function of exposure at 90 K. The heating rate was set at 3 K/s.

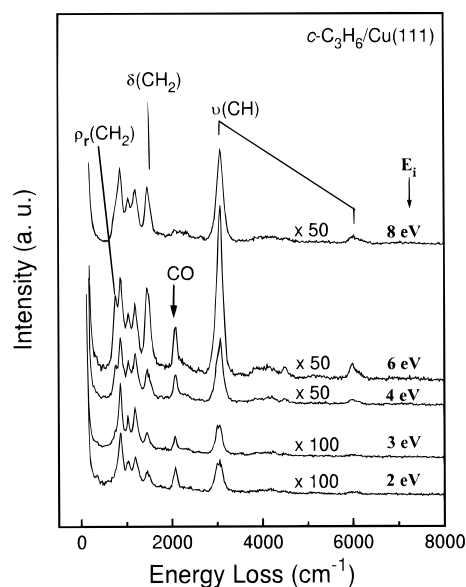


Figure 3. HREELS spectra of cyclopropane on Cu(111) at 90 K for a range of primary beam energies.

2 langmuirs, indicating that multilayer formation does not occur at 90 K. Furthermore, the vibrational frequencies are constant, within the resolution of the instrument, as a function of exposure. That is, there is no indication of chemisorption at low coverages followed by a more weakly bound state at higher coverages. The close match between the gas²⁰ and adsorbed phase vibrational frequencies (Table 1) confirms that cyclopropane is weakly adsorbed on Cu(111). These conclusions are borne out by the TPD data displayed in Figure 2. The integrated area of the desorption peak saturates at an exposure of 2 langmuirs further ruling out the formation of multilayer cyclopropane. In summary, cyclopropane adsorbs weakly at all coverages on Cu(111), and multilayer formation does not occur at 90 K.

HREELS spectra recorded at six different impact energies, over the range of 2.0–8.0 eV, are presented in Figure 3. These spectra display a clear dependence on the primary electron energy. Note, for example, that the first CH stretching overtone feature is barely visible at primary energies of 2.0–3.0 eV; however, its intensity increases to 6 eV and then decreases again. The same comment applies for the loss at 759 cm^{-1} . In Figure 3, this lowest frequency loss is only clearly visible in the spectra recorded at 4 and 6 eV. The loss intensities, normalized to the elastic peak intensity, of all the peaks increase as the primary

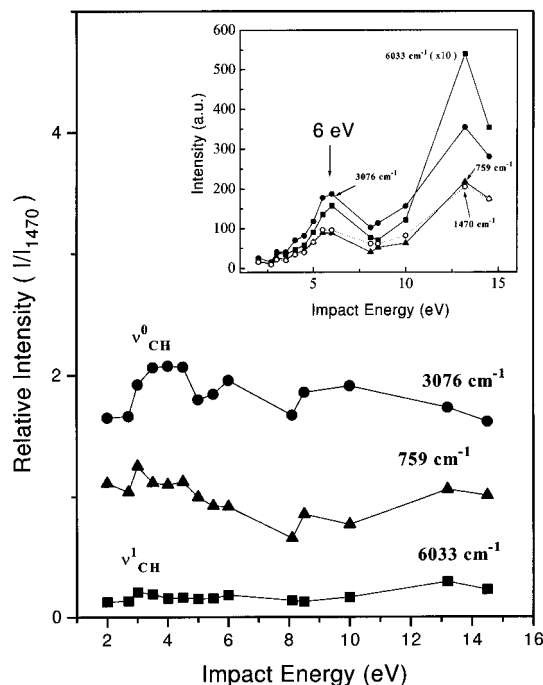


Figure 4. Vibrational excitation functions for selected loss features, all of which are assigned in the text to CH_2 group modes. The excitation spectra displayed in the insert are normalized with respect to the elastic peak intensity. The excitation spectra displayed in the main body of the figure are normalized with respect to the intensity of the CH_2 scissors mode at 1470 cm^{-1} .

energy is raised to 6.0 eV. However, the increase is most pronounced for the CH stretching fundamental and overtone bands. There is also a strong enhancement of the CH_2 scissors band at 1470 cm^{-1} and the feature at 759 cm^{-1} . The losses at 872 , 1034 , and 1179 cm^{-1} are much less enhanced. An analysis of these trends must be made in terms of appropriately normalized excitation functions, such as those shown in Figures 4 and 5. Details of the normalization procedure are given in the Discussion. In brief, the latter two figures show that there is a preferential enhancement of the band intensity of certain modes at 6 eV. They also show that there is a very strong enhancement of all of the observed modes in the 10–15 eV range. The latter enhancement will not be discussed in this paper since no clear resonant structure is resolved in the internally normalized excitation functions above 8 eV. However, as shown elsewhere,¹⁷ dissociative processes resulting in the formation of new surface species take place at approximately 10 and above 15 eV.

Discussion

The HREELS spectrum in Figure 1 displays six losses which may be assigned to fundamental modes, and several losses which may be assigned to overtone or combination bands. As discussed below, the assignment of the losses given in Table 1 is made by taking into account the impact energy dependent data shown in Figures 4 and 5. Primary beam energy dependence in HREELS spectroscopy arises from the energy dependence of the various excitation mechanisms, from the energy dependence of the surface reflectivity and from factors related to the transmission of the spectrometer.²¹ The cross-section for long-range dipolar scattering displays an E^{-1} dependence, with the scattered electrons concentrated in a lobe close to the specular direction. The angular spread is given by $E_1/2E_0$, where E_1 is the loss energy and E_0 is the primary beam energy. Since the analyzer entrance slits in HREELS spec-

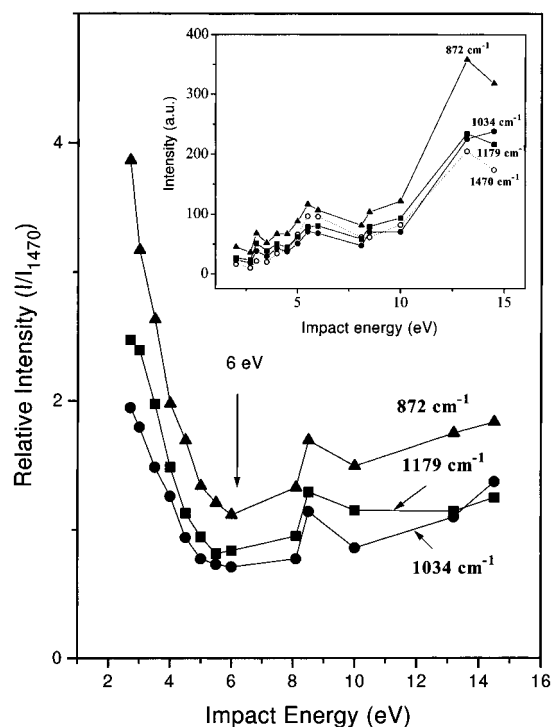


Figure 5. Vibrational excitation functions for cyclopropane on Cu(111). The three modes are assigned in the text to ring vibrations. The normalization procedure is the same as that described for Figure 4.

trometers are by necessity narrow, the dipolar scattering intensity for a given loss typically displays an initial increase in the low-impact energy range. Thus, for example, the CO stretching and metal–carbon stretching loss peaks for CO on Cu(100) reach their respective maxima at impact energies of approximately 4 and 1 eV.²² The data in Figures 4 and 5 are not consistent with dipolar scattering since all of the excitation functions exhibit a maximum at 6 eV, irrespective of their loss energies. In contrast, resonance scattering through temporary negative ion formation displays a number of features which distinguish it from dipolar or impact scattering. First, resonance scattering produces structure in vibrational excitation functions at an energy related to the acceptor level into which electron capture occurs. Second, the excitation of overtone or combination vibrations is one of the manifestations of shape resonance formation. Overtone excitation arises because transient electron capture results in the movement of nuclei on the negative ion potential surface. Autodetachment of the captured electron then typically leads to a vibrationally excited ground state of the neutral molecule. The number of harmonics excited depends on the lifetime of the negative ion and on the details of the negative ion and ground state potential energy surfaces involved.¹⁴ In the present case, the excitation function for the first CH stretching overtone feature suggests the formation of a shape resonance at 6 eV. The fact that only a very weak second overtone feature is observed indicates that the lifetime of the negative ion state is short.

Taken together, Figures 4 and 5 display excitation functions for all of the observed fundamentals and the first CH stretch overtone of cyclopropane on Cu(111). Loss intensities normalized to the elastic peak intensity are shown in the inserts to both figures, whereas the results displayed in the main parts of the figures were obtained by normalizing with respect to the intensity of the loss at 1470 cm^{-1} . Although normalization with respect to the elastic peak will reveal resonance structure, some of the structure in the excitation function may be unrelated to

resonance formation. Most notably, the elastic peak intensity depends on the reflectivity of the surface, whereas resonance scattering does not, since it is not a simple forward scattering process as in the case of dipolar scattering.²¹ Hence, it is necessary to verify whether the structure is also present in internally normalized vibrational excitation functions such as those shown in the main parts of Figures 4 and 5. The latter, internal normalization allows a comparison of relative excitation functions of the different loss features, and it also helps to cancel out structure arising from the reflectivity of the metal surface. The internal normalization is performed with respect to the ν_2 (CH₂ scissor) mode, because it is centrally situated in the fundamental spectrum. The latter point is of potential importance given the $E_i/2E_0$ dependence of the angular spread of the dipolar lobe combined with the limited acceptance angle of the spectrometer. However, in the present experiment, the influence of the latter two factors is small. This is because, firstly, the acceptance angle of the DC-HREELS spectrometer is large (5°), and, secondly, off-specular measurements taken at 10 eV show that nondipolar scattering dominates.²³

A comparison of the EELS data with infrared spectroscopy data for gas phase²⁰ cyclopropane, as given in Table 1, shows that the spectrometer resolution of 40–64 cm⁻¹ is not sufficient for resolving and thus unambiguously assigning all of the six observed loss features. However, the fact that the vibrational excitation functions show that the losses can be divided into two distinct families serves as an aid in assigning them. That is, the excitation functions shown in Figure 4 are relatively constant as a function of primary beam energy, whereas those shown in Figure 5 display structure in the 3–8 eV region. It is clear from Table 1 that the two families of losses shown in Figures 4 and 5 may be plausibly assigned to CH and CC (or ring) vibrations, respectively. The broad loss feature at 3076 cm⁻¹ clearly arises from one or more of the CH stretching modes. The first and second CH stretching overtone features are observed (Figure 1) at 6026 and approximately 8820 cm⁻¹, respectively. The loss at 759 cm⁻¹, which grows in with increasing impact energy (in the 2–6 eV range), may be uniquely attributed to the ν_{14} CH₂ twisting/rocking mode. The 1470 cm⁻¹ loss peak arises from either or both of the ν_2 and ν_9 CH₂ scissors modes. If we assume that the second family of modes are CC or ring vibrations, then they may be assigned as follows. The loss at 1186 cm⁻¹ is the ν_3 ring breathing mode, the loss at 872 cm⁻¹ is the ν_{11} symmetric ring deformation mode, and the loss at 1034 cm⁻¹ is the ν_{10} asymmetric ring deformation/CH₂ wag mode. The assignment of the six loss peaks is in close agreement with that proposed by Felter *et al.* for *c*-C₃H₆ on Ru(0001).⁸ However, the ν_{14} mode (759 cm⁻¹), visible in our spectra, was not resolved in their study, possibly because their spectra were taken at an electron impact energy of 4 eV. The present results show that the loss at 759 cm⁻¹ displays a strong impact energy dependence, at least for the *c*-C₃H₆/Cu(111) system. A feature detected at 570 cm⁻¹ for *c*-C₃H₆ on Ru(001) was not observed for *c*-C₃H₆ on Cu(111). The possible significance of this difference between the ruthenium and copper results is discussed below. The results displayed in the inserts suggest, *but do not prove*, that there is also a weak enhancement of ring modes at 6 eV.

Both the CC and CH excitation functions obtained by normalizing to the elastic peak display a feature consistent with shape resonance formation at 6 eV. The results of the internal normalization against the ν_2 loss intensity confirm both the presence of the resonance and the preferential enhancement of the CH mode intensities. The much weaker enhancement of the ring vibrations results in the negative going structure at 6

eV in the internally normalized excitation functions proper to the ring vibrations (Figure 5). The preferential enhancement of the CH modes is most pronounced for the ν (CH) stretching loss at 3076 cm⁻¹. It then follows that the electron capture giving rise to the resonance at 6 eV occurs into a virtual orbital that displays a node with respect to the CH bond. However, the possibility that ring vibrations are also resonantly excited, albeit to a weaker extent, indicates that the acceptor orbital (assuming only one is involved) is antibonding with respect to both CH and CC. The low-lying unoccupied valence orbitals are as follows; $4a'_1(\sigma^*(\text{CH}_2))$, $2a''_2(\pi^*(\text{CH}_2))$, $4e'(\sigma^*(\text{CH}_2))$, $\sigma^*(\text{CC})$, $1a'_2(\sigma^*(\text{CC}))$, $2e''(\pi^*(\text{CH}_2))$, and $5e'(\sigma^*(\text{CH}_2), \sigma^*(\text{CC}))$.^{24,25} Only the $4e'$ and $5e'$ orbitals are antibonding in both CC and CH. As discussed next, the observed resonance is assigned to $4e'$ by comparison with published *ab initio* orbital calculations²⁴ and with literature data for electron scattering²⁶ and core level excitation studies of gas phase cyclopropane.^{25,27}

Shape resonances in gas phase cyclopropane have been studied by both theoretical^{25,28} and experimental methods.^{25,26} Resonances at 2.6 and 5.5 eV observed in an electron energy loss study by Allan were assigned to electron capture into the $2a''_2$ and $1a'_2$ levels, respectively.²⁶ Both the selective enhancement of CC modes and the f-wave scattering character of the resonance at 5.5 eV supported assignment to $1a'_2$. The $1a'_2$ orbital is purely CC antibonding, hence, the selective excitation of the ν_3 and ν_{11} ring modes. In contrast, the resonance at 2.6 eV led to the selective excitation of the ν_1 , ν_2 , and $\nu_1 + \nu_2$ vibrations consistent with the fact that the $2a''$ orbital is antibonding with respect to the CH and the HH axes. Earlier electron transmission spectroscopy (ETS) work by Howard and Staley²⁴ revealed resonances at 5.5 and 8.5 eV. The resonance at 8.5 eV was attributed to electron capture into the $4e'$ or the $1a'_2$ virtual orbitals; however, Allan's assignment of the resonance at 5.5 eV to $1a'_2$ implies that the resonance at 8.5 eV should be assigned to $4e'$.

An assignment of the shape resonance at 6 eV observed for *c*-C₃H₆ on Cu(111) can be made by a process of elimination. First, one can exclude orbitals which are purely antibonding in CC, given the preferential resonant enhancement of the CH modes. There then remains the $4a'_1$, $2a''_2$, $4e'$, $2e''$, and $5e'$ levels. The electron attachment energy of the $2a''_2$ level of gas phase cyclopropane, as measured by ETS, is 2.6 eV. Thus, an assignment to $2a''_2$ is ruled out since it is highly unlikely that the $2a''_2$ (in *D*_{3h} symmetry) negative ion state would be so greatly destabilized as to appear at 6.0 eV in the weakly adsorbed system. Eliminating $2a''$ in turn rules out an assignment to the LUMO orbital, $4a'_1$, since it lies at even lower energy. Thus, we are left with an assignment to either the $4e'$, the $2e''$, or the higher lying $5e'$ orbitals. *Ab initio* HF/2-31G calculations by Howard and Staley²⁴ place the $2e''$ level at 10.35 eV and the $4e'$ level at 8.21 eV. The latter value is in good agreement with the observation of the $4e'$ resonance at 8.5 eV in gas phase experiments. Thus, in the absence of higher level calculations, the 6 eV resonance is most plausibly assigned to $4e'$. This assignment is also supported by the results of a K-shell electron spectroscopy and multiple scattering X α study by Hitchcock *et al.* of gas phase cyclopropane.²⁷ They assigned a resonance at 2.6 eV above the ionization potential to $4e'$. Since the presence of a core hole in the K-shell experiment contributes a relaxation shift of about 5.0 eV,²⁹ their assignment of the resonance correlates reasonably with the $4e'$ resonance at 8.5 eV revealed by the ETS data of Howard and Staley. Image charge and polarization effects of the order of 1.6 eV³⁰ then partly account for the observation of the $4e'$ resonance at 6.0 eV on the Cu(111) surface. In this context, it is worth noting

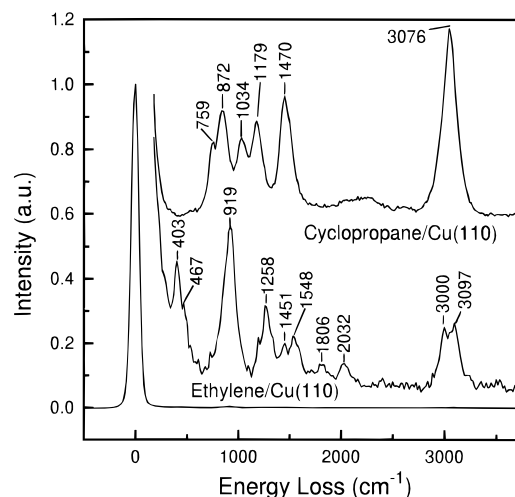
TABLE 2: Correlation Table for D_{3h} Point Group Symmetry

D_{3h}	C_{3v}	$C_s(\sigma_v)$	C_{2v}	$C_s(\sigma_h)$
a'_1	A_1	A'	A_1	A'
a''_2	A_1	A'	B_1	A''
a''_1	A_2	A''	A_2	A''
a'_2	A_2	A''	B_2	A'
e'	E	$A' + A''$	$A_1 + B_2$	A'
e''	E	$A' + A''$	$A_2 + B_1$	A''

that the π^* resonance for benzene on Pt(111) and Pd(111) appear at 2.2–2.6 eV lower in energy than for the gas phase.³¹ The $4e'$ orbitals are antibonding in both CH and CC, and this would account for the resonant excitation of both CH and CC modes. An explanation for the preferential enhancement of the CH vibrations may be given by analogy to isotope effects in the cross-section for dissociative electron scattering experiments.³² For equivalent negative ion potential energy surfaces, the H atoms, as compared to the heavier carbon atoms, suffer greater displacement. Autodetachment, and decay of the negative ion state within the Franck–Condon region, then favors the excitation of CH modes.

The assignment of the resonance to $4e'$ must be consistent with the observed resonant enhancement of vibrational intensities. The selection rule formulated by Wong and Schulz¹⁵ specifies that vibrational modes belonging to the direct product representation of the negative ion state will be resonantly excited. The correlation table for D_{3h} point group symmetry given in Table 2 shows that, for a surface–adsorbate complex displaying C_{2v} or lower symmetry and an e' resonance, only modes belonging to the totally symmetric representation will be excited due to shape resonance formation. Figures 4 and 5 suggest that all of the observed modes draw intensity from the resonance, although there is a clear preferential enhancement of the CH vibrations. Thus, since we can uniquely assign the 759 cm^{-1} loss to the e'' rocking (ν_{14}) mode, its resonant enhancement at 6 eV is consistent with a $C_s(\sigma_v)$ geometry. That is, the e'' mode correlates to an a' mode only through reduction in the point group symmetry to $C_s(\sigma_v)$. Alternatively, if the surface–adsorbate complex displays C_{3v} symmetry, modes belonging to E , A_2 , and A_1 can draw intensity from an E resonance state. Since e'' in D_{3h} symmetry correlates to E in C_{3v} symmetry, the ν_{14} mode would draw intensity from the $4e'$ derived resonance state, as observed. That is, the observed resonant enhancement is consistent with either C_{3v} or $C_s(\sigma_v)$ symmetry.

The similarity between cyclopropane and ethylene was noted in the Introduction, and it is interesting to compare the adsorption of both molecules on copper and ruthenium. A HREELS spectrum for ethylene on Cu(110) is shown in Figure 6. The intense CH_2 wagging (ν_7) loss at 920 cm^{-1} is characteristic of π -adsorbed ethylene.^{33,34} Results from the literature confirm that ethylene π bonds to copper surfaces,³³ whereas a di- σ adsorbed state is formed on Ru(0001).³⁵ In the case of cyclopropane on Ru(0001), Felter *et al.*⁸ pointed out that the experimentally determined $C_s(\sigma_v)$ geometry implied a tilted species with one CC bond parallel to the surface. They further suggested that the chemisorption bond giving rise to this geometry resulted from an interaction between an external $\sigma(\text{CC})$ now nondegenerate HOMO orbital and the metal. It is interesting to note that the HREELS spectra for $c\text{-C}_3\text{H}_6$ on Ru(001) display a loss at 570 cm^{-1} and that this loss is absent in the spectra for cyclopropane on Cu(111). The difference between the two sets of data may be significant with respect to the adsorption geometries of cyclopropane on the ruthenium and copper surfaces. Felter *et al.* assigned the feature at 570

**Figure 6.** Vibrational spectra of cyclopropane and ethylene adsorbed on Cu(110).

cm^{-1} to a mode describing the frustrated translation (T_z) of the molecule against the surface. Further, they attributed the relatively high frequency of this adsorbate–metal mode to mixing with ν_{10} and ν_{11} ring deformation modes as allowed by the low symmetry of the surface complex. Without invoking any arguments based on symmetry, the presence of the mode at 570 cm^{-1} in the $c\text{-C}_3\text{H}_6/\text{Ru}(001)$ spectra and the absence of any mode in the 700–350 cm^{-1} range in the $c\text{-C}_3\text{H}_6/\text{Cu}(111)$ data may suggest that cyclopropane adopts C_{3v} rather than C_s symmetry on Cu(111). That is, we attribute the absence of a high- or medium-frequency T_z loss to a weak nondirectional (i.e., with respect to any individual CC bond) interaction of cyclopropane with the surface of the d^{10} metal. The adsorption geometry on Cu(111) is thus viewed as a π -bonded state with the nonactivated molecule lying flat on the surface. Such a difference in the adsorption symmetry between the two surfaces then reflects a partial activation of cyclopropane by the ruthenium surface. Further activation, as on the reconstructed Ir(110) surface, leads to CC bond cleavage.⁶

Conclusions

Vibrational excitation functions for $c\text{-C}_3\text{H}_6$ on Cu(111) display a shape resonance feature at approximately 6 eV. The resonance is assigned to $4e'$ on the basis of the excitation of both CC and CH modes, and by reference to gas phase electron scattering and *ab initio* studies. The adsorption geometry is either $C_s(\sigma_v)$ or C_{3v} . Complementary HREELS data for ethylene on Cu(111) is used to give preference for a C_{3v} π -bonded geometry.

Notes Added in Proof. Recent results from this group confirm the C_{3v} structure of cyclopropane on Cu(111). This conclusion is based on RAIRS data.

Acknowledgment. Financial support was provided by FCAR and NSERC and Université Laval. R.M. acknowledges the support of an FCAR scholarship for graduate studies. The superb machining skills of André Bouffard and Albert Tremblay are also gratefully acknowledged. Invaluable early advice on the operation of the DC-HREELS instrument was provided by Tom Ellis and Mario Morin.

References and Notes

- (1) Hamilton, J. G.; Palke, W. E. *J. Am. Chem. Soc.* **1993**, *115*, 4159.
- (2) Cremer, D.; Gauss, J. *J. Am. Chem. Soc.* **1986**, *108*, 7467.
- (3) Simon, M. W.; Bennett, C. O.; Suib, S. L. *J. Catal.* **1994**, *148*, 100.

- (4) (a) Wiberg, K. B. *Acc. Chem. Res.* **1996**, 29, 22. (b) Walsh, A. D. *Nature*, **1947**, 159, 712.
- (5) Sheppard, N. *Annu. Rev. Phys. Chem.* **1988**, 39, 589.
- (6) (a) Wittrig, T. S.; Szuromi, P. D.; Weinberg, W. H. *J. Chem. Phys.* **1982**, 102, 716. (b) Kelly, D.; Weinberg, W. H. *J. Chem. Phys.*, **1996**, 105, 7171.
- (7) (a) Son, K.-A.; Gland, J. L. *J. Am. Chem. Soc.* **1995**, 117, 5415. (b) Son, K.-A.; Gland, J. L. *J. Am. Chem. Soc.* **1996**, 118, 10505.
- (8) Hoffmann, F. M.; Felner, T. E.; Weinberg, W. H. *J. Chem. Phys.* **1982**, 76, 3799.
- (9) Lenz-Solomon, P.; Goodman, D. W. *Langmuir* **1994**, 10, 172.
- (10) Leang, P. Ph.D. Thesis, Columbia University, New York, 1994.
- (11) Martel, R.; Rochefort, A.; McBreen, P. H. *J. Am. Chem. Soc.* **1994**, 116, 5965.
- (12) Deleted in proof.
- (13) (a) Palmer, R. E. *Prog. Surf. Sci.* **1992**, 41, 51. (b) Palmer, R. E.; Rous, P. J. *Rev. Mod. Phys.* **1992**, 64, 383.
- (14) (a) Gadzuk, J. W., *J. Chem. Phys.*, **1983**, 79, 3982. (b) Gadzuk, J. W. *Annu. Rev. Phys. Chem.* **1988**, 39, 395.
- (15) Wong, S. F.; Schulz, G. S. *Phys. Rev. Lett.* **1975**, 35, 1429.
- (16) Goldstein, E.; Vijaya, S.; Segal, G. A. *J. Am. Chem. Soc.* **1980**, 102, 6198.
- (17) Martel, R.; McBreen, P. H. Submitted for publication.
- (18) Kevan, S. D.; Dubois, L. H. *Rev. Sci. Instrum.* **1984**, 52, 447.
- (19) Wu, K. L.; Peterson, L. D.; Elliot, G. S.; Kevan, S. D.; Gibson, K. D.; Hinch, B. L.; Dubois, L. H. *Rev. Sci. Instrum.* **1991**, 62, 1256.
- (20) Levin, I. W.; Pearce, R. A. R. *J. Chem. Phys.* **1978**, 69, 2196.
- (21) Ibach, H.; Mills, D. L. *Electron Energy Loss Spectroscopy And Surface Vibrations*; Academic: New York, 1982.
- (22) Anderson, S.; Persson, B. N. J.; Gustafsson, T.; Plummer, E. W. *Solid State Commun.* **1980**, 34, 473.
- (23) Martel, R. Ph.D. Thesis, Université Laval, Québec, Canada, 1995.
- (24) Howard, E.; Staley, S. W. *Resonances In Electron-Molecule Scattering, Van Der Waals Complexes, and Reactive Chemical Dynamics*; Truhlar, D. G., Ed.; ACS Symposium Series 263; American Chemical Society: Washington, DC, 1984; p 183.
- (25) Sze, K. H.; Brion, C. E. *J. Electron Spectrosc. Relat. Phenom.* **1991**, 57, 117.
- (26) (a) Allan, M. *Pure Appl. Chem.* **1995**, 67, 1. (b) Allan, M. *J. Am. Chem. Soc.* **1993**, 115, 641.
- (27) Hitchcock, A. P.; Newbury, D. C.; Oshii, I.; Stöhr, J.; Horsley, J. A.; Redwing, R. D.; Johnson, A. L.; Sette, F. *J. Chem. Phys.* **1986**, 85, 4849.
- (28) Winstead, C.; Sun, Q.; McKoy, V. *J. Chem. Phys.* **1992**, 96, 4246.
- (29) Jones, T. S.; Ashton, M. R.; Richardson, N. V. *J. Chem. Phys.* **1989**, 90, 7564.
- (30) Grudzkov, Y. A.; Watanabe, K.; Sawabe, K.; Matsumoto, Y. *Chem. Phys. Lett.* **1994**, 227, 243.
- (31) Kesmodel, L. L. *Phys. Rev. Lett.* **1984**, 53, 1001.
- (32) Ben Arfa, M.; Edard, F.; Tronc, M. *Chem. Phys. Lett.* **1990**, 167, 602.
- (33) Slater, D. S.; Hollins, P.; Chesters, M. A. *Surf. Sci.* **1994**, 306, 155.
- (34) Jenks, C. J.; Bent, B. E.; Bernstein, N.; Zarra, F. *Surf. Sci.* **1992**, 277, L89.
- (35) Hills, M. M.; Parmeter, J. E.; Mullins, C. B.; Weinert, W. H. *J. Am. Chem. Soc.* **1986**, 108, 3554.